Received: 12 June 2023 | Revised: 15 October 2023 | Accepted: 20 November 2023

DOI: 10.1111/cas.16038

Cancer Science WILEY

ORIGINAL ARTICLE

Histone methyltransferase SUV420H1/KMT5B contributes to poor prognosis in hepatocellular carcinoma

Hirotaka Kato[1] | Shinya Hayami[1] | Masaki Ueno[1] | Norihiko Suzaki[1] | Masashi Nakamura[1] | Tomohiro Yoshimura[1] | Atsushi Miyamoto[1] | Yoshinobu Shigekawa[1] | Ken-Ichi Okada[1] | Motoki Miyazawa[1] | Yuji Kitahata[1] | Shogo Ehata[2] | Ryuji Hamamoto[3] | Hiroki Yamaue[1] | Manabu Kawai[1]

[1]Second Department of Surgery, School of Medicine, Wakayama Medical University, Wakayama, Japan

[2]Department of Pathology, School of Medicine, Wakayama Medical University, Wakayama, Japan

[3]Division of Medical AI Research and Development, National Cancer Center Research Institute, Tokyo, Japan

Correspondence
Shinya Hayami, Wakayama Medical University, 811-1 Kimiidera, Wakayama 641-8509, Japan.
Email: shin-8@wakayama-med.ac.jp

Abstract

Hepatocellular carcinoma (HCC) has a high rate of recurrence and poor prognosis, even after curative surgery. Multikinase inhibitors have been applied for HCC patients, but their effect has been restricted. This study aims to clarify the clinical impact of SUV420H1/KMT5B, one of the methyltransferases for histone H4 at lysine 20, and elucidate the novel mechanisms of HCC progression. We retrospectively investigated SUV420H1 expression using HCC clinical tissue samples employing immunohistochemical analysis ($n = 350$). We then performed loss-of-function analysis of SUV420H1 with cell cycle analysis, migration assay, invasion assay and RNA sequence for Gene Ontology (GO) pathway analysis in vitro, and animal experiments with xenograft mice in vivo. The SUV420H1-high-score group ($n = 154$) had significantly poorer prognosis for both 5-year overall and 2-year/5-year disease-free survival than the SUV420H1-low-score group ($n = 196$) ($p < 0.001$ and $p < 0.05$, respectively). The SUV420H1-high-score group had pathologically larger tumor size, more tumors, poorer differentiation, and more positive vascular invasion than the SUV420H1-low-score group. Multivariate analysis demonstrated that SUV420H1 high score was the poorest independent factor for overall survival. SUV420H1 knockdown could suppress cell cycle from G1 to S phase and cell invasion. GO pathway analysis showed that SUV420H1 contributed to cell proliferation, cell invasion, and/or metastasis. Overexpression of SUV420H1 clinically contributed to poor prognosis in HCC, and the inhibition of SUV420H1 could repress tumor progression and invasion both in vitro and in vivo; thus, further analyses of SUV420H1 are necessary for the discovery of future molecularly targeted drugs.

Abbreviations: ADD, amino-actinomycin D; AFP, alpha-fetoprotein; AFP-L3, the lens culinaris agglutin-reactive fraction of AFP; BrdU, 5′-bromo-2′-deoxyuricine; cDNA, complementary DNA; CRISPR/Cas9, clustered regularly interspaced short palindromic repeats/CRISPR-associated protein 9; CT, computed tomography; DAPI, diamidino-2-phenylindole; DCP, des-γ-carboxy prothrombin; DEGs, differentially expressed genes; DFS, disease-free survival; EGFP, enhanced green fluorescent protein; ERK, extracellular signal-regulated kinase; FACS, fluorescence-activated cell sorting; FBS, fetal bovine serum; FGFR, fibroblast growth factor receptor; GAPDH, glyceraldehyde 3-phosphate dehydrogenase; GFP, green fluorescent protein; GO, Gene Ontology; HBV, hepatitis B virus; HCC, hepatocellular carcinoma; HCV, hepatitis C virus; HDR, homology-directed repair; HE, hematoxylin eosin; ICC, immunocytochemistry; IGFR, insulin-like growth factor receptor; IHC, immunohistochemistry; IRS, immunoreactive scoring system; MRI, magnetic resonance imaging; mRNA, messenger RNA; OS, overall survival; PTMs, post-translational modifications; qRT-PCR, quantitative real-time polymerase chain reaction; SDH, succinate dehydrogenase; siRNA, small interfering RNA; TGF-β, transforming growth factor beta; tRNA, total RNA.

KEYWORDS
hepatocellular carcinoma, methylation, methyltransferase, SUV420H1/KMT5B

1 | INTRODUCTION

Hepatocellular carcinoma (HCC) has a high rate of recurrence and poor prognosis, even after curative surgery.[1] To prolong survival time in patients with unresectable HCC, multikinase inhibitors, such as sorafenib,[2,3] regorafenib,[4] lenvatinib,[5] and cabozantinib[6] in turn, have been applied since 2008; however, it must be noted that their therapeutic effect is restricted.[7] All existing molecularly targeted drugs for HCC thus relied only on phosphorylation; other novel pathways or mechanisms different from antiphosphorylation are therefore needed to prolong the survival for advanced HCC patients. As the crucial role for cancer cell progression, the condensation of chromatin and the regulation of gene expression were influenced also by other post-translational modifications (PTMs) including phosphorylation, methylation, acetylation, ubiquitination, and so on.[8,9] We therefore have especially focused on methylation and reported that several histone methyltransferases/demethylases play vital roles in various types of cancer.[10–18] As one of the contributions to mechanisms for the progression of tumors and interactions between different PTMs, we previously reported that RB1 methylation by histone methyltransferase SMYD2 promoted RB1 phosphorylation and cell cycle progression.[19] Methylation might be therefore suggested to promote phosphorylation through PTMs' interaction; however, the detailed molecular mechanisms through methylation still remain unclear, and further research is needed. This study aims to elucidate the critical roles of SUV420H1/KMT5B (Suppressor Of Variegation 4–20 homolog 1/Lysine Methyltransferase 5B), one of the methyltransferases for histone 4 lysin 20,[20] by expression analysis using clinical HCC tissue samples and loss-of-function analyses using SUV420H1-specific small interfering RNAs (siSUV420H1) in vitro and SUV420H1-specific clustered regularly interspaced short palindromic repeats (CRISPR)/CRISPR-associated protein 9 (Cas9) system in vivo.

2 | MATERIALS AND METHODS

This study was designed and carried out in accordance with the Declaration of Helsinki following a study protocol approved by Research Ethics Comittee of Wakayama Medical University (approval number: 2521).

2.1 | Patients

This study enrolled 350 patients who underwent initial hepatectomy for HCC at Wakayama Medical University Hospital between January 2000 and December 2014.

2.2 | Postoperative follow-up for HCC patients

Blood examination including tumor markers for HCC were conducted every 3 months for 5 years after surgery. Contrast-enhanced computed tomography (CT) or magnetic resonance imaging (MRI) were conducted every 3 months for 2 years after surgery, and then every 6 months thereafter.

2.3 | Adjuvant chemolipiodolization

From January 2000 to March 2005, HCC patients who underwent initial hepatectomy did not receive adjuvant chemotherapy. Between April 2005 and December 2010, HCC patients who underwent initial hepatectomy routinely received adjuvant chemolipiodolization using 40 mg of epirubicin and 6 mg of mitomycin C. From January 2011, 140 mg of miriplatin was used for adjuvant chemolipiodolization at 3 months after surgery.[21] As a special note, between September 2012 and December 2016, three rounds of scheduled adjuvant chemolipiodolization were administered at 3, 6, and 12 months after surgery as clinical trial.[22]

2.4 | Hematoxylin and eosin staining

Any tumor tissues including background liver were fixed in 4% paraformaldehyde at room temperature. The tissues were treated with xylene at room temperature and rehydrated with 100% ethanol. The tissue sections were put into hematoxylin staining solution at room temperature, rinsed with distilled water, and washed with PBS buffer; then, the tissue sections were put into eosin staining solution at room temperature. The tissue sections were sequentially dehydrated in 100% ethanol and then subjected to xylene, dried at 65°C, and sealed with neutral gum.

2.5 | Immunohistochemistry (IHC)

The tumors included well, moderately, and poorly differentiated hepatocellular carcinoma (Table 1). Tissue sections, including both liver tumor and corresponding background liver, were randomly selected. Slides with paraffin-embedded HCC specimens were deparaffinized with xylene and rehydrated with 100% ethanol. The slides were processed under high pressure (95°C for 10 min) in target retrieval solution citrate pH 6 (Dako) and, subsequently, 0.3% hydrogen peroxide (H_2O_2). After being treated with serum-free ready-to-use protein block (Dako), the slides were incubated overnight at 4°C with a rabbit anti-SUV420H1 polyclonal antibody

TABLE 1 Patients' characteristics between the SUV420H1-high-score and -low-score groups.

Variables	SUV420H1-low-score group ($N = 196$)	SUV420H1-high-score group ($N = 154$)	p-Value
Age (years)	70 (33–88)	70 (38–89)	0.84
Sex			
Male	157	109	0.063
Female	39	45	
Alcohol history			
Yes	92	57	0.066
No	104	97	
HBV-Ag			
Positive	167	25	0.59
Negative	29	129	
HCV-Ab			
Positive	94	93	0.086
Negative	102	61	
Child-Pugh grade			
A	184	140	0.31
B	12	14	
AFP (ng/mL)	14.5 (1.3–41299)	46.0 (1.2–148196)	**0.024**
AFP-L3 (%)	11.7 (0.6–96.5)	26.0 (0.5–95.6)	0.071
DCP (mIU/mL)	171 (8.1–1410815)	775.5 (2.3–693070)	0.38
Tumor size (cm)	3.5 (1.0–20)	5.3 (1.1–20)	**0.021**
Tumor number			
Single	152	91	**0.003**
Multiple	44	63	
Differentiation			
Well or moderately	169	117	**0.043**
Poorly	27	37	
Vascular invasion			
Positive	57	62	**0.038**
Negative	139	92	
Fibrosis stage			
F4	82	84	**0.042**
F0-3	114	70	
Activity stage			
A2-3	66	54	0.29
A0-1	130	100	
Adjuvant chemolipiodolization			
Yes	130	97	0.61
No	66	57	

Note: Bold values indicate statistical significance.

Abbreviations: AFP, alpha-fetoprotein; AFP-L3, the lens culinaris agglutin-reactive fraction of AFP; DCP, des-γ-carboxy prothrombin; HBV, hepatitis B virus; HCV, hepatitis C virus.

(LS-C815054; LifeSpan BioSciences) at 1:1000 dilution ratio or a rabbit anti-E-cadherin polyclonal antibody (#3195; Cell Signaling) at 1:400 dilution ratio. The slides were reacted with anti-rabbit EnVision HRP (Dako) and stained with Histofine DAB substrate kit (Nichirei) and Mayer's hematoxylin solution (Fujifilm, Tokyo, Japan). The IHC staining result was evaluated with immunoreactive scoring system (IRS) as follows[23]; the number of positive cells was scaled (0: no positive cells; 1: 1%–25% positive cells; 2: 25%–50% positive cells; 3: 51%–75% positive cells; 4: 76%–100% positive cells), and the intensity of positive cells was also scaled (0: negative; 1: weak;

2: moderate; 3: strong). When there were areas with a variety of staining intensities, the most predominant intensity was selected. The number of positive cell scores was multiplied by the intensity of positive cell scores. IHC staining was scored by four investigators including liver surgeons (HK, NS, and MN) and a pathologist (SE). The evaluation was performed without the knowledge of clinical and pathological variables. When the scoring evaluation differed, a thorough discussion was conducted about the scoring to reach consensus. The cutoff value was set where the area under the curve met the highest value.

2.6 | Cell lines and cultures

Three human hepatic carcinoma cell lines, Huh-7 (RRID: CVCL_0336; derived from the primary tumor of a male with HCC) that was obtained from JCRB Cell Bank, SNU475 (RRID: CVCL_0497; derived from the primary tumor of a male patient with HCC) that was obtained from ACTT, and HepG2 (RRID: CVCL_0027; derived from the primary tumor of a male patient with HCC) that was obtained from JCRB Cell Bank, were used in these experiments. These cell lines were authenticated using STR profiling. Huh-7 and HepG2 cells were cultured in Dulbecco's modified Eagle's medium (Thermo Fisher Scientific), and SNU475 cell was cultured in RPMI-1640 medium (Thermo Fisher Scientific) supplemented with 10% fetal bovine serum (FBS). These cells were incubated at 37°C with 5% CO_2 condition. All experiments were performed with mycoplasma-free cells.

2.7 | Transfection with small interfering RNA

Small interfering RNA (siRNA) oligonucleotide duplexes (Merck-Sigma-Aldrich) were customized and synthesized for targeting the human SUV420H1 transcripts. Using the siRNA oligonucleotide duplexes as negative control, enhanced green fluorescent protein (siEGFP) was also customized and synthesized. The siRNA sequences are shown in Table S1. The siRNA duplexes (100 nM final concentration) were transfected to HCC cells with Lipofectamine RNAiMAX (Thermo Fisher Scientific) according to the manufacturer's protocol.

2.8 | Quantitative real-time polymerase chain reaction (qRT-PCR)

Specific primers for all human glyceraldehyde 3-phosphate dehydrogenase (GAPDH, housekeeping gene), succinate dehydrogenase (SDH, housekeeping gene), and SUV420H1 were constructed for qRT-PCR (Table S2). Total RNA (tRNA) was extracted from HCC cells after being treated with siRNA (20 nM) with the RNeasy Micro Kit (QIAGEN). Complementary DNA (cDNA) was then constructed using SuperScript III RT (Thermo Fisher Scientific). SsoAdvanced Universal SYBR Green Supermix (Bio-Rad Laboratories), forward and reverse primers (50 nM final concentration), and reversely transcribed cDNA were added. The qRT-PCRs were performed with CFX96 touch (Bio-Rad Laboratories) as described in the manufacturer's protocol, and the expression level of messenger RNA (mRNA) was analyzed by ΔCT method.[24] The experiment was done in triplicate.

2.9 | Cell proliferation assay

Hepatocellular carcinoma cells of 1.0×10^4 per well in a 96-well plate were pre-incubated for 24 h. Subsequently, Cells were transfected with siRNAs for 24–48 h, and Cell Counting Kit-8 (DOJINDO) was applied as described in the manufacturer's protocol. Absorbance was measured with a microplate reader (SH-9000; Corona Electric) at 450 nm. The experiment was done in triplicate.

2.10 | Immunocytochemistry

Hepatocellular carcinoma cells of 5.0×10^4 per well in a six-well plate were fixed with 4% paraformaldehyde. Subsequently, Cells were treated with serum-free ready-to-use protein block (Dako) and then incubated overnight with rabbit anti-SUV420H1 polyclonal antibody (LS-C359286; LifeSpan BioSciences) at 1:200 dilution ratio at 4°C. Cells were stained with anti-rabbit EnVision HRP (Dako) and Histofine DAB substrate kit (Nichirei). The experiment was done in triplicate.

2.11 | Cell cycle analysis

Hepatocellular carcinoma cells of 5×10^5 per well in six-well plates were pre-incubated for 24–48 h. Subsequently, Cells were treated with siRNA (20 nM) in Opti-MEM reduced serum medium (Thermo Fisher Scientific) for 24–48 h, followed by labeling with 10 μM 5′-bromo-2′-deoxyuricine (BrdU) of the BrdU flow kit (BD Pharmingen). After collection, Cells were fixed and permeabilized with buffer and incubated with DNase at 37°C. Cells were treated with FITC-conjugated anti-BrdU antibody (BD Pharmingen) at 1:50 dilution. Cells were washed, and total DNA was stained with 7-amino-actinomycin D (7-ADD; 20 μL/well), followed by flow cytometry analysis with fluorescence-activated cell sorting (FACS) Calibur (BD Pharmingen) and MultiCycle for Macintosh software (BD Pharmingen). The experiment was done in triplicate.

2.12 | Wound-healing assay

Hepatocellular carcinoma cells of 1.5×10^4 were pre-incubated in a Culture-insert 2 Well 24 silicon plate with a gap of 500 ± 50 μm, (ibidi GmbH) in six-well plates for 24–48 h following the manufacturer's

protocol. The silicon plate was then removed, and siRNAs were added to each well. Cell migration was monitored under stable pressure of 5% CO_2 in air at 37°C and recorded every 6 h for 48 h using Digital sight DS-L1 (Nikon). The area of the remaining gap was measured with software Fiji/ImageJ (https://imagej.net/software/fiji/). The experiment was done in triplicate.

2.13 | Cell invasion assay

The ability of HCC cell invasion was examined using CytoSelect 24-well Cell Invasion Assay (CBA-110; Cell Biolabs). Cells of 1.5×10^5 treated with siRNA (20 nM) were seeded into the upper chamber with Opti-MEM, and culture medium was applied to the lower chamber. Cells were allowed to invade from the upper chamber toward the lower chamber. The medium was then discarded, Cell Stain Solution (part no. 11002; Cell Biolabs) was added inside the upper chamber, and the stained Cells were observed under microscopy. Extraction solution (part no. 11003; Cell Biolabs) was then added inside the lower chamber. Absorbance was measured with a microplate reader (SH-9000; Corona Electric) at 560 nm. The experiment was done in triplicate.

2.14 | Differentially expressed genes (DEGs) and Gene Ontology (GO) pathway analysis using RNA sequence

After treatment with siRNA, tRNA was extracted from HCC cells with the Rneasy Micro Kit (QIAGEN). A single library was then constructed with TruSeq Stranded Total RNA (Illumina) and Illumina's NovaSeq 6000 (Macrogen Inc.) according to protocols (Cancer Precision Medicine). Cytoscape (RRID: SCR_003032) was applied to build a network for DEGs between siSUV420H1 and siEGFP (cutoff; twofold and $p<0.05$). Next, we applied ClueGo, a plug-in of Cytoscape, to perform GO pathway analysis (http://geneontology.org/).

2.15 | Animal experiments

All animal procedures were performed based on the recommendations of the Guide for Care and Use of Laboratory Animals (National Research Council). This study was approved by Animal Facility Committee of Wakayama Medical University (approval number: 1119).

2.16 | Transfection with CRISPR/Cas9 to HCC cells

Gene transfer and editing were performed with CRISPR/Cas9-based gene-editing technology. Commercially available SUV420H1 CRISPR/Cas9 knockout (KO) plasmid (sc-404615; Santa Cruz Biotechnology), SUV420H1 homology-directed repair (HDR) plasmid (sc-404615-HDR; Santa Cruz Biotechnology), and Control CRISPR/Cas9 plasmid (sc-418922; Santa Cruz Biotechnology) as negative control were transfected to HCC cells (Huh-7 and HepG2) with UltraCruz transfection reagent (sc-395739; Santa Cruz Biotechnology) following the manufacturer's protocol, and then subjected to selection by 1 μg/mL puromycin (sc-108071; Santa Cruz Biotechnology) for 24 h prior to qRT-PCR, immunofluorescence, and injection into mice. The experiment was done in triplicate.

2.17 | Immunofluorescence

Hepatocellular carcinoma cells of 2.0×10^5 treated with CRISPR/Cas9 and puromycin in six-well plates were fixed with 4% paraformaldehyde and stained with 4′,6-diamidino-2-phenylindole (DAPI, DOJINDO) at 1:1000 ratio. Cells were observed with a fluorescence microscope BZ-X800 (Keyence). The experiment was done in triplicate.

2.18 | Human liver cancer xenograft

All animal experiments were performed with 6-week-old athymic nude mice (BALB/cSlc-nu/nu: Japan SLC). For tumor injection, HCC cells of 1.0×10^6 with SUV420H1 CRISPR/Cas9 KO plasmid and SUV420H1 HDR plasmid (CRISPR/Cas9 SUV420H1 KO) were suspended with 70 μL of growth medium and 200 μL of MatriMix (Nippi) following the manufacturer's protocol. HCC cells of 1.0×10^6 with control CRISPR/Cas9 plasmid (CRISPR/Cas9 control) were similarly suspended. The solution of 200 μL containing HCC cells was then subcutaneously injected into the right lateral back of mice. The tumor size was measured every 7 days with calipers, and estimated tumor volumes were calculated with a formula:

$$\left(\text{width}^2\times\text{length}\right)/2.$$

All mice were sacrificed at 28 days after the inoculation, and the size of resected tumors was recorded. The experiment was done in triplicate.

2.19 | Statistical analysis

Patient characteristics and laboratory data were analyzed using Fisher's exact test and the Mann–Whitney *U* test. Overall survival curve and disease-free survival curve were analyzed by the Kaplan–Meier method and log-rank test. Risk factors for overall survival and disease-free survival were analyzed using the Cox proportional hazards model. Statistical significance was defined as $p<0.05$. All statistical analyses were performed with JMP Pro 16.0 (SAS Institute).

3 | RESULTS

3.1 | High expression of SUV420H1 was associated with poor prognosis

In the tumor tissue, the nuclei of tumor cells were stained weakly, moderately, or strongly, while in the non-tumor tissue there was no or very weak staining. Representative IRS and scoring distribution of the 350 cases of HCC are shown in Figure 1 and Figure S1A. SUV420H1-high (IRS ≥4; $n=154$) and -low-score groups (IRS ≤3; $n=196$) were classified according to cutoff value where the area under the curve showed the highest value (Figure S1B). Regarding patients' characteristics, the SUV420H1-high-score group had larger tumor size, greater number of tumors, poorer differentiation, more vascular invasion, and more fibrous stage in the background liver compared with the SUV420H1-low-score group (Table 1). In 2- and 5-year disease-free survival (DFS) after surgery, the SUV420H1-high-score group had poorer prognosis than the SUV420H1-low-score group (Figure 2A; 2-year DFS: 38.3% vs. 59.0%, 5-year DFS: 18.1% vs. 36.3%, respectively). In 5-year overall survival (OS) after surgery, the SUV420H1-high-score group similarly had poorer prognosis than the SUV420H1-low-score group (Figure 2B; 5-year OS: 33.8% vs. 64.3%). In view of evaluating the prognostic factors for DFS and OS, univariate analysis for DFS revealed that alpha-fetoprotein (AFP) >20 ng/mL, tumor size >5 cm, multiple tumors, poorer differentiation, positive vascular invasion, and SUV420H1 high score were risk factors, and multivariate analysis for DFS revealed that multiple tumors and positive vascular invasion were independent factors (Table 2). On the other hand, univariate analysis for OS revealed that AFP >20 ng/mL, tumor size >5 cm, multiple tumors, positive vascular invasion, adjuvant chemolipiodolization, and SUV420H1 high score were risk factors, and multivariate analysis for OS revealed that SUV420H1 high score was the most significant independent factor (Table 3). To elucidate the importance of SUV420H1, we additionally investigated recurrent or metastatic patterns. The SUV420H1-high-score group had more intrahepatic lesions and more patients with extrahepatic lesions than the SUV420H1-low-score group in recurrent or metastatic patterns (Table 4).

3.2 | SUV420H1 regulated HCC cells progression, migration, and invasion

We performed loss-of-function analysis with SUV420H1-specific siRNAs (siSUV420H1#1 and #2) and siEGFP as negative control. The siRNAs were transected into three HCC cell lines: Huh-7, SNU475, and HepG2. After the treatment with siRNA, qRT-PCR showed that mRNA expression levels were significantly decreased in siSUV420H1 compared with those in siEGFP (Figure 3A and Figure S2A,B). Immunocytochemistry (ICC) and cell proliferation

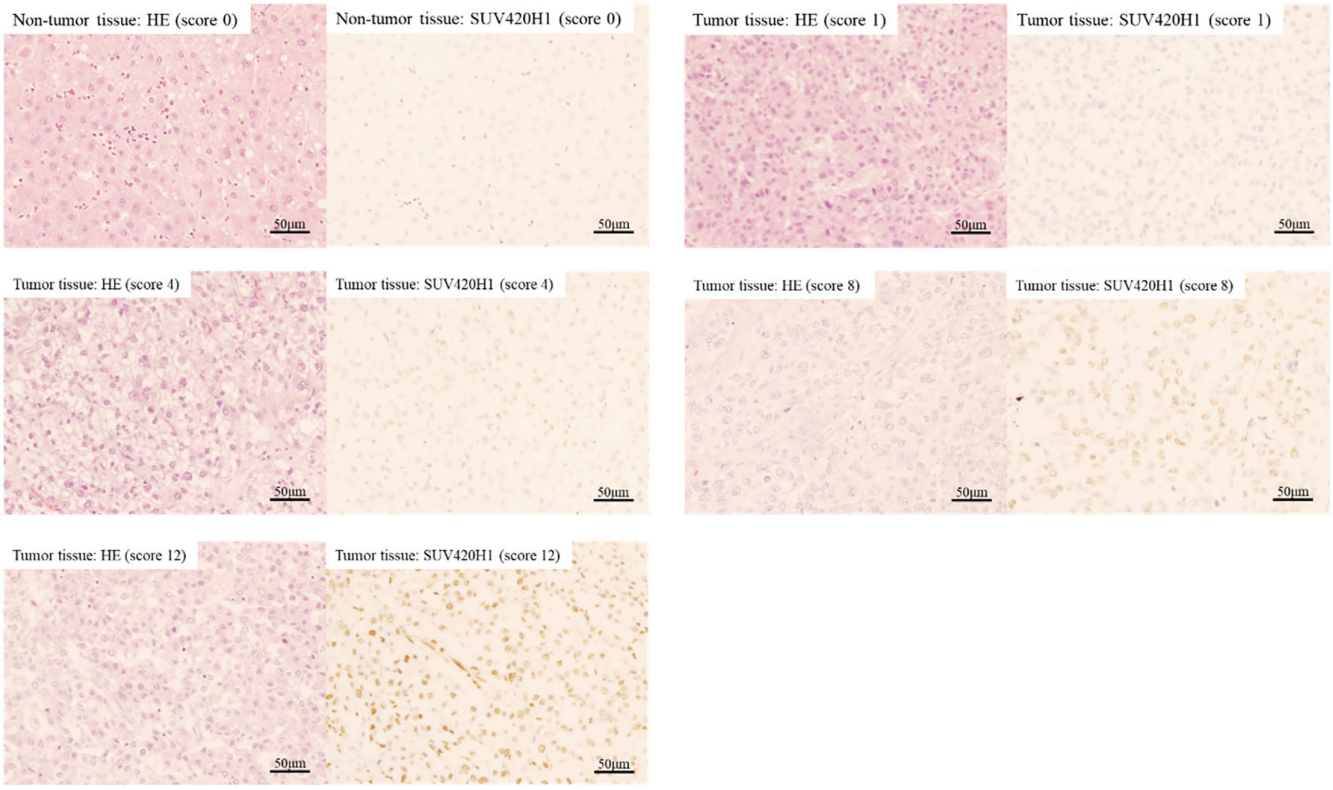

FIGURE 1 Immunohistochemical analysis using hepatocellular carcinoma (HCC) and corresponding background (non-tumor) liver. Immunohistochemical classification based on the staining pattern according to immunoreactive scoring system in tumor and nontumor tissues.

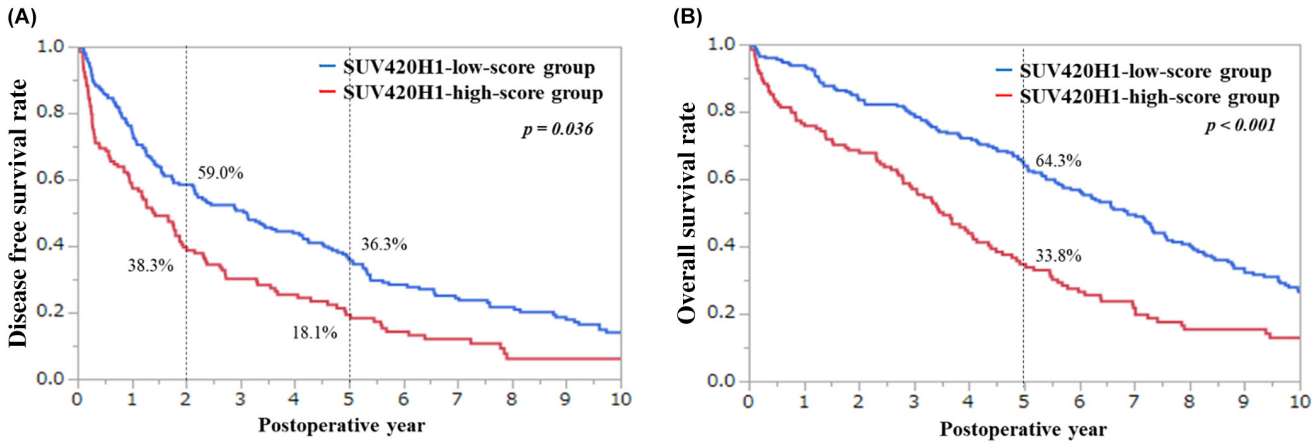

FIGURE 2 Disease-free and overall survival for hepatocellular carcinoma (HCC) between the SUV420H1-high-score and -low-score groups. (A) Disease-free survival curve in the SUV420H1-high-score and -low-score groups. (B) Overall survival curve in the SUV420H1-high-score and -low-score groups. *p*-Values were calculated using the log-rank test.

analysis also showed that HCC cells were significantly decreased in siSUV420H1 compared with those in siEGFP (Figure 3B,C and Figure S3). To validate the detailed mechanism behind SUV420H1 inhibition of cell proliferation or growth, we performed cell cycle analysis using flow cytometry. The proportion of S phase was significantly decreased in siSUV420H1 compared with that in siEGFP, while the proportion of G1 phase was significantly increased in siSUV420H1 compared with that in siEGFP. Conversely, the proportion of sub-G1 and G2/M phases did not show statistically significant difference between siEGFP and siSUV420H1 (Figure 3D,E and Figure S4). SUV420H1 is indicated to be linked to the progress of cell cycle from G1 to S phase rather than apoptosis. To evaluate the migration and invasion ability, we performed a wound-healing assay and a cell invasion assay. In the wound-healing assay, the gap area was significantly more slowly filled up in siSUV420H1 than that in siEGFP (Figure 4A,B and Figure S5). In the cell invasion analysis, the number of cells that invaded into the membrane was significantly decreased in siSUV420H1 compared with siEGFP (Figure 4C,D and Figure S6).

3.3 | SUV420H1 was associated with cell proliferation signal pathways

To better understand the pathways associated with SUV420H1, we silenced SUV420H1 in Huh-7 cells not derived from hepatitis virus (nBnC) HCC and SNU475 cells derived from hepatitis B virus (HBV) HCC and then performed RNA sequence and GO pathway analysis using Cluego software in Cytoscape. In Huh-7 cells, within the DEGs, a total of 1003 dysregulated genes, including 604 upregulated and 399 downregulated genes were identified between siEGFP or siSUV420H1-transfected cells. GO analysis showed that SUV420H1 mainly contributed to cell proliferation pathways, such as extracellular signal-regulated kinase (ERK), transforming growth factor beta receptor (TGF-β), and fibroblast growth factor receptor (FGFR). SUV420H1 also contributed to cell adhesion by cadherin, cell activity, histone modification, and metabolism (Figure 5A). In SNU475 cells, within the DEGs, a total of 799 dysregulated genes, including 472 upregulated and 327 downregulated genes were identified between siEGFP or siSUV420H1-transfected cells. SUV420H1 contributed to cell proliferation pathways, such as extracellular signal-regulated kinase (ERK), fibroblast growth factor receptor (FGFR), and insulin-like growth factor receptor (IGFR). SUV420H1 also contributed to cell adhesion by cadherin, cell activity, histone modification, morphogenesis, and infection immunity (Figure 5B). Moreover, common DEGs in Huh-7 and SNU475 cells were a total of 120 dysregulated genes, including 90 upregulated and 30 downregulated genes. SUV420H1 commonly contributed to cell proliferation pathways, such as extracellular signal-regulated kinase (ERK) and fibroblast growth factor receptor (FGFR), and cell adhesion by cadherin (Figure 5C).

3.4 | SUV420H1 high expression could be involved in attenuating E-cadherin expression

Gene Ontology pathway analysis showed SUV420H1 was also involved in cell adhesion by cadherin. Therefore, we examined additional IHC with anti-E-cadherin antibody to evaluate the relationship between SUV420H1 and E-cadherin using HCC-resected specimens. The SUV420H1-high-expression specimens showed E-cadherin expression could be attenuated (Figure 6A,B); on the other hand, some SUV420H1-low-expression specimens showed E-cadherin expression could not be attenuated (Figure 6C,D).

3.5 | CRISPR/Cas9 SUV420H1 KO inhibited tumor proliferation in HCC xenograft mice

SUV420H1 knockdown with siRNAs was confirmed to inhibit cell progression in vitro, so we next performed in vivo examination using xenograft HCC tumors in athymic nude mice with CRISPR/Cas9

TABLE 2 Univariate and multivariate analysis for disease-free survival.

	Univariate analysis			Multivariate analysis		
Variables	HR	95% CI	*p*-Value	HR	95% CI	*p*-Value
Sex						
Female	1		0.67			
Male	1.12	0.664–1.895				
Age (year)						
<65	1		0.48			
≥65	1.18	0.737–1.910				
HBV-Ag						
Negative	1		0.64			
Positive	1.16	0.617–2.182				
HCV-Ab						
Negative	1		0.44			
Positive	1.19	0.756–1.882				
Alcohol history						
No	1		0.43			
Yes	1.20	0.759–1.908				
Child-Pugh						
A	1		0.52			
B	1.34	0.543–3.316				
AFP (ng/mL)						
≤20	1		**0.043**	1		0.55
>20	1.68	1.243–2.295		1.36	0.538–1.562	
AFP-L3 (%)						
≤10	1		0.25			
>10	1.34	0.815–2.210				
DCP (mIU/mL)						
≤40	1		0.47			
>40	1.22	0.700–2.151				
Triple positive[a]						
No	1		0.16			
Yes	1.44	0.868–2.380				
Tumor size (cm)						
≤5	1		**0.035**	1		0.94
>5	1.36	1.034–1.798		1.12	0.741–1.393	
Tumor number						
Single	1		**<0.001**	1		**<0.001**
Multiple	2.43	1.359–4.368		1.82	1.290–2.687	
Differentiation						
Well or moderately	1		**0.042**	1		0.67
Poorly	1.39	1.006–1.936		1.23	0.947–1.687	
Vascular invasion						
Negative	1		**<0.001**	1		**0.039**
Positive	1.87	1.334–2.809		1.42	1.032–1.967	

TABLE 2 (Continued)

	Univariate analysis			Multivariate analysis		
Variables	HR	95% CI	*p*-Value	HR	95% CI	*p*-Value
Adjuvant chemolipiodolization						
No	1		0.11			
Yes	0.63	0.432–1.086				
SUV420H1						
Low score	1		**0.036**	1		0.88
High score	1.35	0.799–1.931		1.10	0.699–1.711	

Note: Bold values indicate statistical significance.

Abbreviations: AFP, alpha-fetoprotein; AFP-L3, the lens culinaris agglutin-reactive fraction of AFP; DCP, des-γ-carboxy prothrombin; HBV, hepatitis B virus; HCV, hepatitis C virus; HR, hazard ratio.

[a]All of AFP, AFP-L3, and DCP are positive.[25]

SUV420H1 KO and CRISPR/Cas9 Control in Huh-7 and HepG2 cells. SUV420H1 and HDR genes were confirmed to be cotransfected into HCC cell nucleus in immunofluorescence analysis (Figure 7A and Figure S7A), and mRNA expression level was confirmed to be significantly decreased in CRISPR/Cas9 SUV420H1 KO compared with that in CRISPR/Cas9 control (Figure 7B and Figure S7B). Tumor growth was significantly inhibited in CRISPR/Cas9 SUV420H1 KO compared with that in CRISPR/Cas9 control (Figure 7C,D and Figure S7C,D).

3.6 | CRISPR/Cas9 SUV420H1 KO could increase E-cadherin expression in HCC xenograft mice tumor

We demonstrated that SUV420H1 high expression could be involved in the attenuation of E-cadherin in IHC using HCC-resected specimens. Then, we performed additional IHC using SUV420H1 KO and control tumors resected from HCC xenograft mice in Huh-7 and HepG2 cells. The control tumor highly expressed with SUV420H1 had no expression of E-cadherin (Figure S8A,B); on the other hand, the SUV420H1 KO tumor expressed E-cadherin at cell membrane (Figure S8C,D).

4 | DISCUSSION

Current clinical analyses demonstrated that the SUV420H1-high-score group had pathologically advanced status, such as larger tumor size, a larger rate of multiple tumors, poorer differentiation, and more positive vascular invasion than the SUV420H1-low-score group. Moreover, the SUV420H1-high-score group had significantly poorer DFS and OS than the SUV420H1-low-score group. In multivariate analysis for DFS and OS, SUV420H1 high score was an independent factor for OS, but not a factor for DFS. The SUV420H1-high-score group had more intrahepatic lesions and more patients with extrahepatic metastasis, which led to poorer prognosis. In the loss-of-function analysis, siSUV420H1 could certainly suppress mRNA expression level and HCC cell proliferation through the inhibition of transition from G1 to S phase in the cell cycle. Vougiouklakis et al. also reported that SUV420H1 promoted the transition from G1 to S phase in head and neck squamous carcinoma cells,[26] and Wu et al.[27] also reported that SUV420H1 promotes the transition from G1 to S phase by repressing p21 in chronic myeloid leukemia cells. Our cell cycle analysis results and these previous reports supported clinical data that the SUV420H1-high-score group had larger tumor size. Moreover, the ability of migration and invasion was significantly inhibited with siSUV420H1. E-cadherin could be downregulated by SUV420H1 because DEG analysis clarified that E-cadherin was significantly increased in siSUV420H1 compared with siEGFP. Reduced expression of E-cadherin increases invasion or metastasis of tumor cells in HCC.[28] During the process of epithelial–mesenchymal transition (EMT) in promoting invasion or metastasis of many epithelium-derived carcinomas including HCC,[29] epithelial cells actively downregulate cell–cell adhesion, lose polarity, and acquire a mesenchymal phenotype that enables tumor cells to invade surrounding tissues and to metastasize in distant lesion.[30] GO analysis also showed that SUV420H1 had a pathway associated with cell adhesion by cadherin. Indeed, the tumors that highly expressed SUV420H1 did not express E-cadherin; on the other hand, the tumors with low expression of SUV420H1 expressed E-cadherin at cell membrane in IHC using HCC-resected specimens. In the same way, the tumors highly expressing SUV420H1 (control) did not express E-cadherin; on the other hand, the tumors with SUV420H1 KO expressed E-cadherin at cell membrane using tumors resected from HCC xenograft mice. SUV420H1 could therefore contribute to cell invasion or metastasis, although there have been no reports on the association of SUV420H1 with invasion or metastasis through E-cadherin. The current GO pathway analysis revealed pathways associated with oncology including phosphorylation terms, such as ERK, FGFR, TGFβ, and IGFR, which were essential for carcinogenesis or tumor progression.[31–34] Vougiouklakis et al.[26] also reported that phosphorylation of nonhistone protein ERK could be enhanced through SUV420H1 methylation. Protein methylation by SUV420H1 could also be associated with progression mechanisms in HCC through phosphorylation, similar to a previous report.[19]

TABLE 3 Univariate and multivariate analysis for overall survival.

	Univariate analysis			Multivariate analysis		
Variables	HR	95% CI	*p*-Value	HR	95% CI	*p*-Value
Sex						
Female	1		0.92			
Male	1.03	0.627–1.476				
Age (year)						
<65	1		0.97			
≥65	1.01	0.629–1.608				
HBV-Ag						
Negative	1		0.53			
Positive	0.83	0.462–1.289				
HCV-Ab						
Negative	1		0.18			
Positive	1.33	0.872–1.841				
Alcohol history						
No	1		0.30			
Yes	1.25	0.817–1.813				
Child-Pugh						
A	1		0.11			
B	1.92	0.858–4.312				
AFP (ng/mL)						
≤20	1		**<0.001**	1		0.13
>20	2.25	1.468–3.073		1.49	0.893–2.507	
AFP-L3 (%)						
≤10	1		0.45			
>10	1.19	0.756–1.872				
DCP (mIU/mL)						
≤40	1		0.21			
>40	1.38	0.832–2.300				
Triple positive[a]						
No	1		0.35			
Yes	1.24	0.786–1.754				
Tumor size (cm)						
≤5	1		**0.035**	1		0.38
>5	1.60	1.030–2.100		1.28	0.269–2.243	
Tumor number						
Single	1		**<0.001**	1		0.29
Multiple	2.67	1.659–3.657		1.42	0.692–3.014	
Differentiation						
Well or moderately	1		0.15			
Poorly	1.49	0.865–2.126				
Vascular invasion						
Negative	1		**<0.001**	1		0.65
Positive	2.16	1.364–2.912		1.17	0.588–2.348	

TABLE 3 (Continued)

	Univariate analysis			Multivariate analysis		
Variables	**HR**	**95% CI**	***p*-Value**	**HR**	**95% CI**	***p*-Value**
Adjuvant chemolipiodolization						
No	1		**0.012**	1		0.49
Yes	0.55	0.354–0.883		0.77	0.409–1.534	
SUV420H1						
Low score	1		**<0.001**	1		**<0.001**
High score	5.31	3.330–7.459		4.29	2.451–9.103	

Note: Bold values indicate statistical significance.

Abbreviations: AFP, alpha-fetoprotein; AFP-L3, the lens culinaris agglutin-reactive fraction of AFP; DCP, des-γ-carboxy prothrombin; HBV, hepatitis B virus; HCV, hepatitis C virus; HR, hazard ratio.

[a]All of AFP, AFP-L3, and DCP are positive.[25]

TABLE 4 Recurrent or metastatic pattern in the SUV420H1-high-score and -low-score groups.

	SUV420H1-low-score group (*N* = 196)	**SUV420H1-high-score group (*N* = 154)**	***p*-Value**
Intrahepatic lesion (single/multiple)	95/18	21/74	**<0.001**
Extrahepatic lesion	11	38	**<0.001**

Note: Bold values indicate statistical significance.

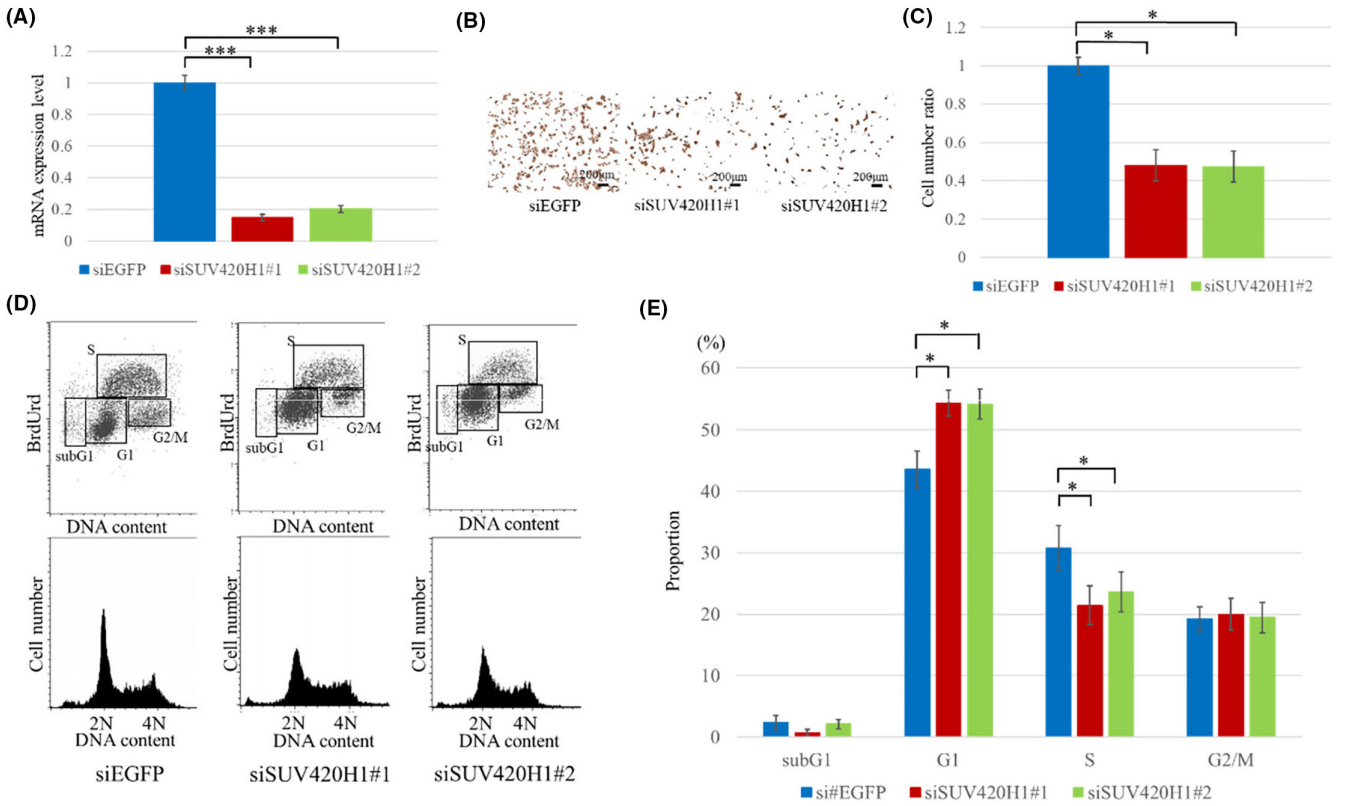

FIGURE 3 Cell progression analysis using small interfering RNA (siRNA) specific for SUV420H1 in Huh-7. (A) The relative mRNA expression levels by quantitative real-time polymerase chain reaction in siEGFP and siSUV420H1. (B, C) Immunocytochemistry and cell proliferation analysis in siEGFP and siSUV420H1. (D, E) Cell cycle analysis with flow cytometry and proportion of cell cycle phase in siEGFP and siSUV420H1. Results are presented as mean ± SEM. $^{*}p < 0.05$, $^{***}p < 0.001$. All the experiments were done in triplicate.

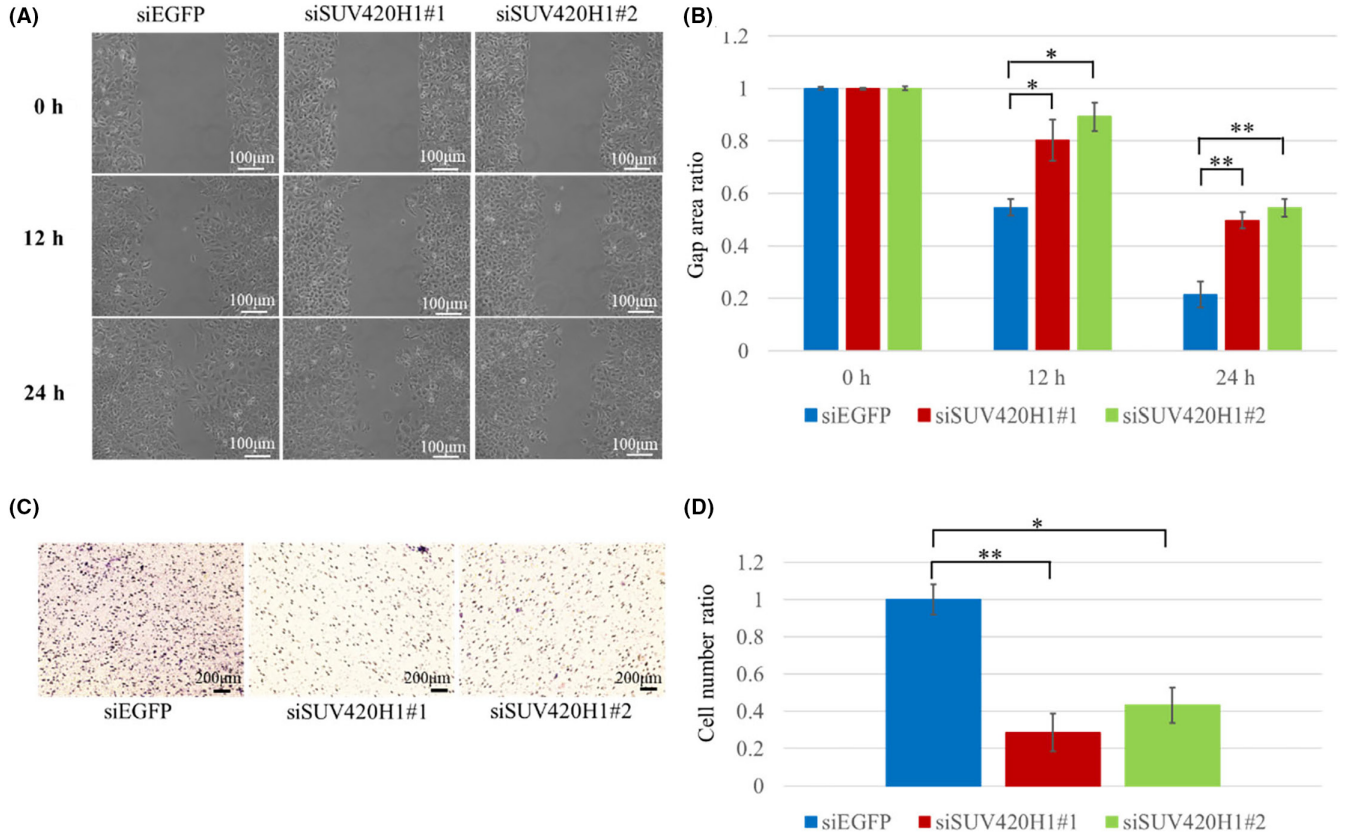

FIGURE 4 Cell migration and cell invasion analysis using small interfering RNA (siRNA) specific for SUV420H1 in Huh-7. (A, B) Gap area at 0, 12, and 24 h in wound-healing assay using siEGFP and siSUV420H1. (C, D) Cell number ratio that invaded into membrane in cell invasion analysis using siEGFP and siSUV420H1. Results are presented as mean ± SEM. $^{*}p < 0.05$, $^{**}p < 0.01$. All the experiments were done in triplicate.

High expression of SUV420H1 has been reported in cases of breast cancer[35] but not in other types of cancer. This is the first report to describe the important contribution of SUV420H1 to HCC. In the biological analyses, a small number of reports stated that histone methylation by SUV420H1 has association with cell cycle progression, DNA damage check point mechanism, and regulation of gene expression through conversion of the nucleosome structure.[36,37] Meanwhile, non-histone protein methylations are categorized into five different functions: other protein modification in which methylation subsequently evokes phosphorylation, protein–protein interaction in which methylation regulates interactions, protein stability in which methylation inhibits polyubiquitylation, subcellular localization in which methylation regulates localization between the nucleus and the cytoplasm, and promotor binding in which methylation promotes transcription factors.[38] Regarding SUV420H1 as a non-histone methylation target, only methylation of lysine 302 and 361 on ERK has been reported.[26] The function or role of SUV420H1, however, has not been sufficiently elucidated. SUV420H1 might have other non-histone methylation candidates, so further analysis is required to clarify the novel mechanism and pathways for tumor growth or metastasis in detail. Instead, the present GO pathway analysis had some terms such as cell activity, histone modification, metabolism, and infection-immunity, which were important functions for cancer growth and progression as downstream of SUV420H1, so further analyses of each individual function are necessary. We could demonstrate that SUV420H1 knockdown could suppress tumor growth in vivo. This will be a first step in the discovery of anticancer drugs related to protein methylation, as tazemetostat, an inhibitor of EZH2, has been clinically applied for lymphoma.[39]

In conclusion, overexpression of SUV420H1 could clinically contribute to poor prognosis in HCC. The inhibition of SUV420H1 could inhibit tumor progression and invasion both in vitro and in vivo; thus, further analyses of SUV420H1 are necessary for discovering future molecularly targeted drugs.

FIGURE 5 Pathways associated with SUV420H1 using Gene Ontology (GO) analysis. (A) GO terms involving SUV420H1 in Huh-7 cell line that were derived neither from hepatitis B virus (HBV) nor C virus (HCV) (nBnC) hepatocellular carcinoma (HCC). GO enriched in siSUV420H1-transfected cells, compared with siEGFP-transfected cells, are indicated. (B) GO terms involving SUV420H1 in SNU475 cell line of HBV-derived HCC. Gene ontologies enriched in siSUV420H1-transfected cells, compared with siEGFP-transfected cells, are indicated. (C) Common GO terms in Huh-7 and SNU475 cell lines.

(A) GO terms in siSUV420H1-transfected cells compared with siEGFP-trasfected cells in Huh-7

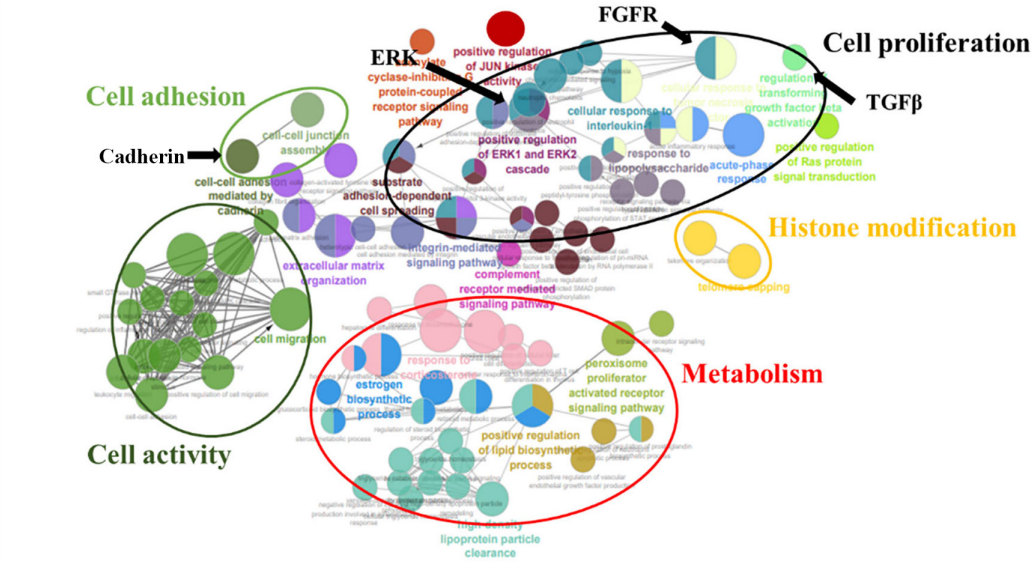

(B) GO terms in siSUV420H1-transfected cells compared with siEGFP-trasfected cells in SNU475

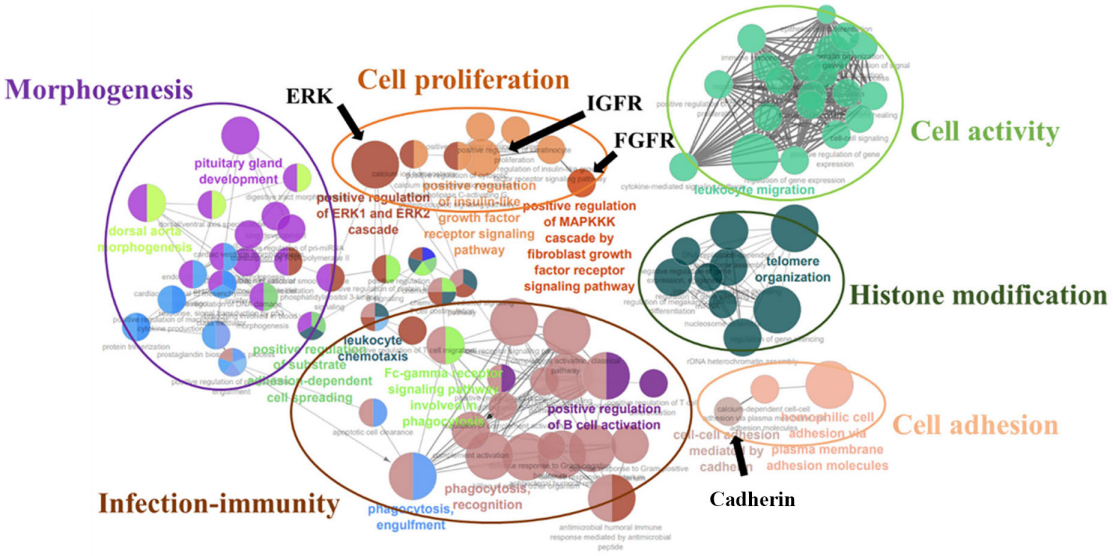

(C) Common GO terms with siSUV420H1-tranfected cells in Huh-7 and SNU475

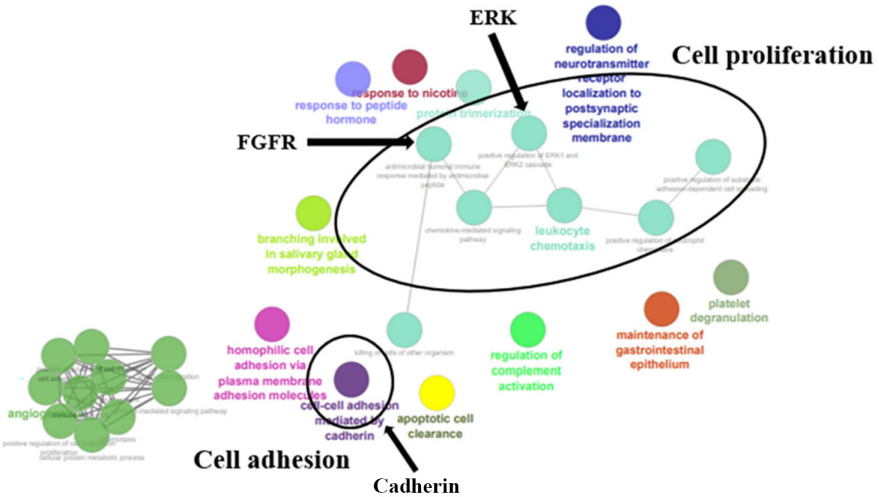

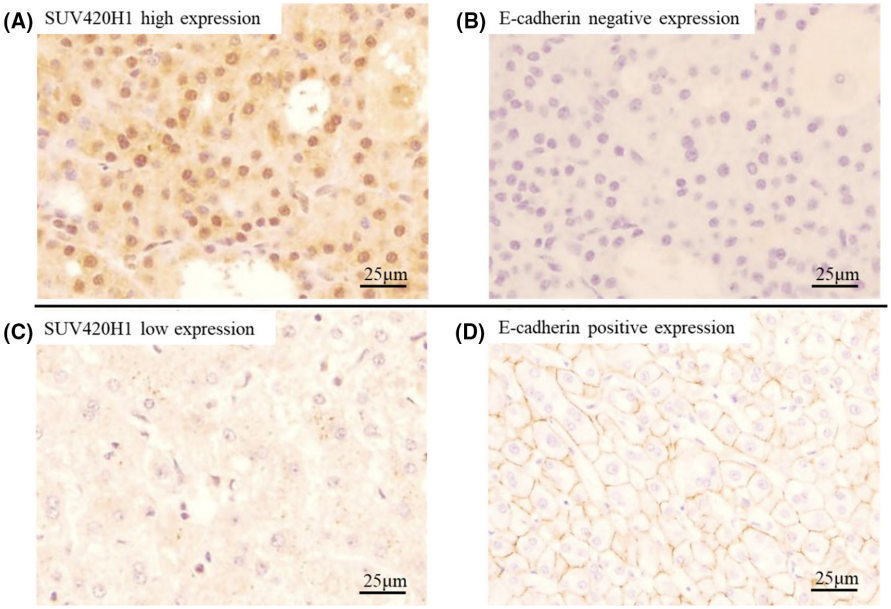

FIGURE 6 Immunohistochemistry with anti-E-cadherin antibody to evaluate the relationship between SUV420H1 and E-cadherin using hepatocellular carcinoma (HCC)-resected specimens. (A, B) The relationship between SUV420H1 high expression and E-cadherin expression. (C, D) The relationship between SUV420H1 low expression and E-cadherin expression.

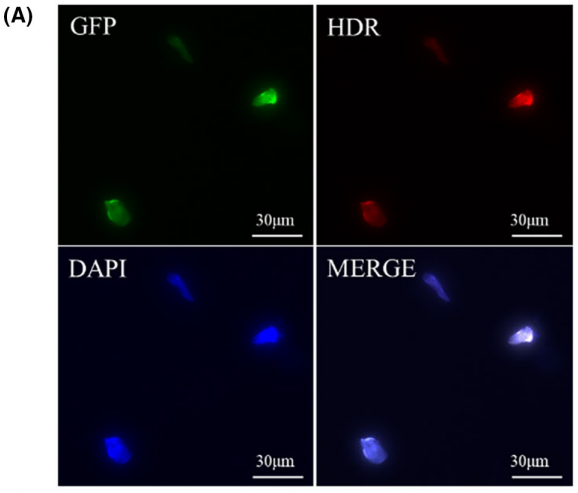

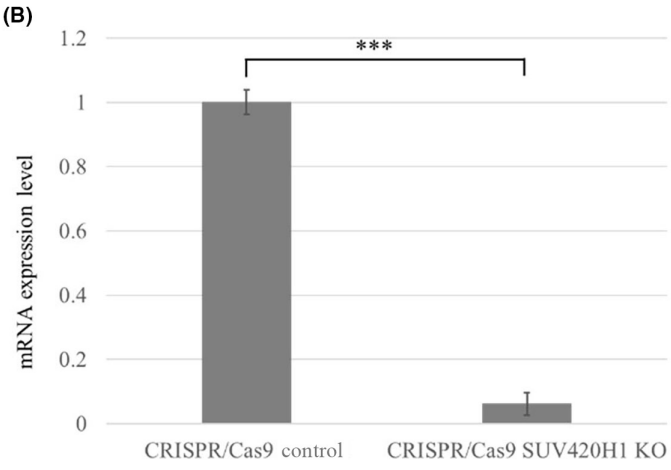

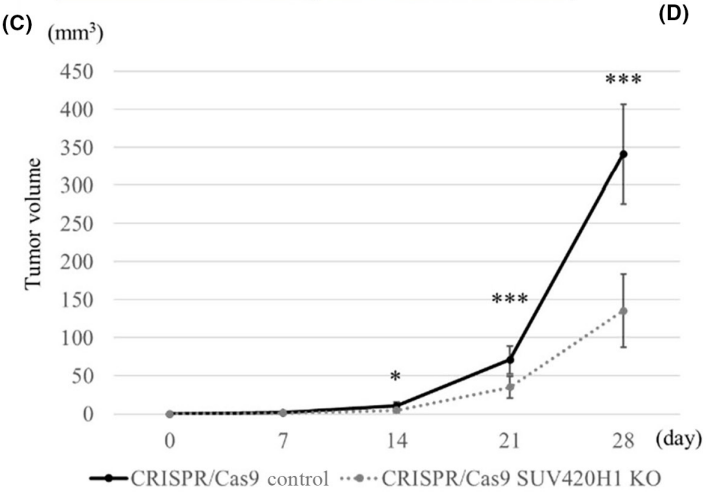

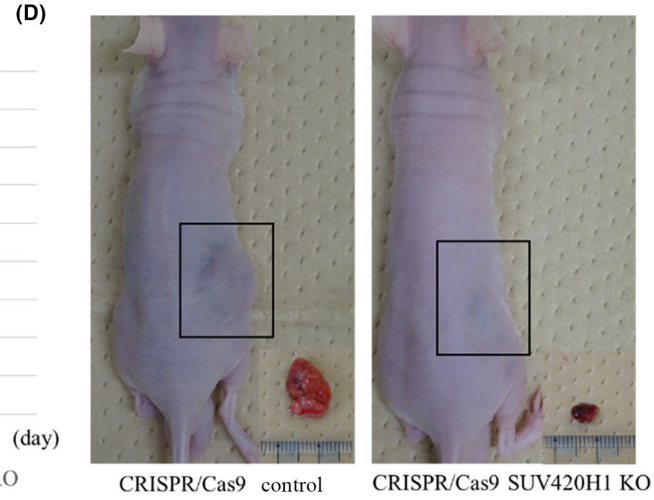

FIGURE 7 In vivo examination employing xenograft hepatocellular carcinoma (HCC) tumors using CRISPR/Cas9 specific for SUV420H1 in Huh-7. (A) Immunofluorescence for SUV420H1 and HDR genes cotransfected into Huh-7 cell nucleus. (B) The relative mRNA expression level in CRISPR/Cas9 control and CRISPR/Cas9 SUV420H1 KO. (C) The changeover time of tumor progression in CRISPR/Cas9 control and CRISPR/Cas9 SUV420H1 KO. (D) Photographs of subcutaneous tumor and macroscopic specimens on day 28. Scale bars, 30 μm. DAPI, diamidino-2-phenylindole; GFP, green fluorescent protein; HDR, homology-directed repair. Results are presented as mean ± SEM. $^{*}p < 0.05$, $^{***}p < 0.001$. All the experiments were done in triplicate.

AUTHOR CONTRIBUTIONS

Hirotaka Kato: Data curation; formal analysis; investigation; methodology; writing – original draft. **Shinya Hayami:** Conceptualization; methodology; project administration. **Masaki Ueno:** Data curation; methodology. **Norihiko Suzaki:** Data curation; methodology. **Masashi Nakamura:** Data curation; methodology. **Tomohiro Yoshimura:** Data curation; methodology. **Atsushi Miyamoto:** Data curation; methodology. **Yoshinobu Shigekawa:** Data curation; methodology. **Ken-Ichi Okada:** Data curation; methodology. **Motoki Miyazawa:** Data curation; methodology. **Yuji Kitahata:** Data curation; methodology. **Shogo Ehata:** Formal analysis; investigation; methodology; supervision. **Ryuji Hamamoto:** Supervision. **Hiroki Yamaue:** Supervision. **Manabu Kawai:** Supervision.

ACKNOWLEDGMENTS

We acknowledge proofreading and editing by Benjamin Phillis at the Clinical Study Support Center at Wakayama Medical University.

CONFLICT OF INTEREST STATEMENT

Ryuji Hamamoto is an editorial board member of *Cancer Science*. Ryuji Hamamoto declares conflict of interest for the present article. The other authors declare no conflict of interest for the present article.

DATA AVAILABILITY STATEMENT

Data sharing is not applicable to the present article because no datasets were generated or analyzed during the current study. All clinical data and images adopted in this article are contained in the medical records of Wakayama Medical University.

ETHICS STATEMENT

Approval of the Research Protocol by an Institutional Reviewer Board: This study was approved by Research Committee of Wakayama Medical University (approval number: 2521).

Informed Consent: N/A.

Registry and the Registration No. of the Study/Trial: N/A.

Animal Studies: All animal procedures were performed based on the recommendations of the Guide for Care and Use of Laboratory Animals (National Research Council). This study was approved by Animal Facility Committee of Wakayama Medical University (approval number: 1119).

ORCID

Hirotaka Kato https://orcid.org/0000-0002-7068-6509

Shinya Hayami https://orcid.org/0000-0002-4177-6281

REFERENCES

1. Lee SC, Tan HT, Chung MC. Prognostic biomarkers for prediction of recurrence of hepatocellular carcinoma: current status and future prospects. *World J Gastroenterol*. 2014;20(12):3112-3124.
2. Llovet JM, Ricci S, Mazzaferro V, et al. Sorafenib in advanced hepatocellular carcinoma. *N Engl J Med*. 2008;359(4):378-390.
3. Cheng AL, Kang YK, Chen Z, et al. Efficacy and safety of sorafenib in patients in the Asia-Pacific region with advanced hepatocellular carcinoma: a phase III randomised, double-blind, placebo-controlled trial. *Lancet Oncol*. 2009;10(1):25-34.
4. Bruix J, Qin S, Merle P, et al. Regorafenib for patients with hepatocellular carcinoma who progressed on sorafenib treatment (RESORCE): a randomized, double-blind, placebo-controlled, phase 3 trials. *Lancet*. 2017;389(10064):56-66.
5. Kudo M, Finn RS, Qin S, et al. Lenvatinib versus sorafenib in first-line treatment of patients with unresectable hepatocellular carcinoma: a randomised phase 3 non-inferiority trial. *Lancet*. 2018;391(10126):1163-1173.
6. Kelley RK, Ryoo BY, Merle P, et al. Second-line cabozantinib after sorafenib treatment for advanced hepatocellular carcinoma: a subgroup analysis of the phase 3 CELESTIAL trial. *ESMO Open*. 2020;5(4):e000714.
7. Huang A, Yang XR, Chung WY, Dennison AR, Zhou J. Targeted therapy for hepatocellular carcinoma. *Signal Transduct Target Ther*. 2020;5(1):146.
8. Martin C, Zhang Y. The diverse functions of histone lysine methylation. *Nat Rev Mol Cell Biol*. 2005;6(11):838-849.
9. Xu H, Wu M, Ma X, Huang W, Xu Y. Function and mechanism of novel histone posttranslational modifications in health and disease. *Biomed Res Int*. 2021;2021:6635225.
10. Cho HS, Kelly JD, Hayami S, et al. Enhanced expression of EHMT2 is involved in the proliferation of cancer cells through negative regulation of SIAH1. *Neoplasia*. 2011;13(8):676-684.
11. Cho HS, Suzuki T, Dohmae N, et al. Demethylation of RB regulator MYPT1 by histone demethylase LSD1 promotes cell cycle progression in cancer cells. *Cancer Res*. 2011;71(3):655-660.
12. Yoshimatsu M, Toyokawa G, Hayami S, et al. Dysregulation of PRMT1 and PRMT6, type I arginine methyltransferases, is involved in various types of human cancers. *Int J Cancer*. 2011;128(3):562-573.
13. Cho HS, Shimazu T, Toyokawa G, et al. Enhanced HSP70 lysine methylation promotes proliferation of cancer cells through activation of Aurora kinase B. *Nat Commun*. 2012;3:1072.
14. Takawa M, Cho HS, Hayami S, et al. Histone lysine methyltransferase SETD8 promotes carcinogenesis by deregulating PCNA expression. *Cancer Res*. 2012;72(13):3217-3227.
15. Cho HS, Toyokawa G, Daigo Y, et al. The JmjC domain-containing histone demethylase KDM3A is a positive regulator of the G1/S transition in cancer cells via transcriptional regulation of the HOXA1 gene. *Int J Cancer*. 2012;131(3):E179-E189.
16. Shigekawa Y, Hayami S, Ueno M, et al. Overexpression of KDM5B/JARID1B is associated with poor prognosis in hepatocellular carcinoma. *Oncotarget*. 2018;9(76):34320-34335.
17. Hayami S, Yoshimatsu M, Veerakumarasivam A, et al. Overexpression of the JmjC histone demethylase KDM5B in human carcinogenesis: involvement in the proliferation of cancer cells through the E2F/RB pathway. *Mol Cancer*. 2010;9:59.

18. Hayami S, Kelly JD, Cho HS, et al. Overexpression of LSD1 contributes to human carcinogenesis through chromatin regulation in various cancers. *Int J Cancer*. 2011;128(3):574-586.
19. Cho HS, Hayami S, Toyokawa G, et al. RB1 methylation by SMYD2 enhances cell cycle progression through an increase of RB1 phosphorylation. *Neoplasia*. 2012;14(6):476-486.
20. Yang H, Pesavento JJ, Starnes TW, et al. Preferential dimethylation of histone H4 lysine 20 by Suv4-20. *J Biol Chem*. 2008;283(18):12085-12092.
21. Ueno M, Uchiyama K, Ozawa S, et al. Adjuvant chemolipiodolization reduces early recurrence derived from intrahepatic metastasis of hepatocellular carcinoma after hepatectomy. *Ann Surg Oncol*. 2011;18(13):3624-3631.
22. Ueno M, Hayami S, Kawai M, et al. Prognostic impact of adjuvant chemolipiodolization and treatment frequency on patients with hepatocellular carcinoma after hepatectomy: prospective study with historical control group. *Surg Oncol*. 2021;36:99-105.
23. Aigelsreiter A, Ress AL, Bettermann K, et al. Low expression of the putative tumour suppressor spinophilin is associated with higher proliferative activity and poor prognosis in patients with hepatocellular carcinoma. *Br J Cancer*. 2013;108(9):1830-1837.
24. Silver N, Best S, Jiang J, Thein SL. Selection of housekeeping genes for gene expression studies in human reticulocytes using real-time PCR. *BMC Mol Biol*. 2006;7:33.
25. Kiriyama S, Uchiyama K, Ueno M, et al. Triple positive tumor markers for hepatocellular carcinoma are useful predictors of poor survival. *Ann Surg*. 2011;254(6):984-991.
26. Vougiouklakis T, Sone K, Saloura V, et al. SUV420H1 enhances the phosphorylation and transcription of ERK1 in cancer cell. *Oncotarget*. 2015;6(41):43162-43171.
27. Wu Y, Wang Y, Liu M, et al. SUV420H1 promotes G1 to S phase transition by downregulating p21 WAF1/CIP1 expression in chronic myeloid leukemia K562 cells. *Oncol Lett*. 2018;15(5):6123-6130.
28. Matsumura T, Makino R, Mitamura K. Frequent down-regulation of E-cadherin by genetic and epigenetic changes in the malignant progression of hepatocellular carcinomas. *Clin Cancer Res*. 2001;7(3):594-599.
29. Arias AM. Epithelial mesenchymal interactions in cancer and development. *Cell*. 2001;105(4):425-431.
30. He X, Chen Z, Jia M, Zhao X. Downregulated E-cadherin expression indicates worse prognosis in Asian patients with colorectal cancer: evidence from meta-analysis. *PloS One*. 2013;8(7):e70858.
31. Guo YJ, Pan WW, Liu SB, Shen ZF, Xu Y, Hu LL. ERK/MAPK signaling pathway and tumorigenesis. *Exp Ther Med*. 2020;19(3):1997-2007.
32. Ahmad I, Iwata T, Leung HY. Mechanism of FGFR-mediated carcinogenesis. *Biochim Biphys Acta*. 2012;1823(4):850-860.
33. Goulet CR, Pouliot F. TGFβ signaling in the tumor microenvironment. *Adv Exp Med Biol*. 2021;1270:89-105.
34. Hua H, Kong Q, Yin J, Zhang J, Jiang Y. Insulin-like growth factor receptor signaling in tumorigenesis and drug resistance: a challenge for cancer therapy. *J Hematol Oncol*. 2020;13(1):64.
35. Liu L, Kimball S, Liu H, Holowatyj A, Yang ZQ. Genetic alterations of histone lysine methyltransferase and their significance in breast cancer. *Oncotarget*. 2015;6(4):2466-2482.
36. Schübeler D, MacAlpine DM, Scalzo D, et al. The histone modification pattern of active genes revealed through genome-wide chromatin analysis of a higher eukaryote. *Genes Dev*. 2004;18(11):1263-1271.
37. Wang Z, Zang C, Rosenfeld JA, et al. Combinatorial patterns of histone acetylations and methylations in the human genome. *Nat Genet*. 2008;40(7):897-903.
38. Hamamoto R, Saloura V, Nakamura Y. Critical roles of non-histone protein lysine methylation in human tumorigenesis. *Nat Rev Cancer*. 2015;15(2):110-124.
39. von Keudell G, Salles G. The role of tazemetostat in relapsed/refractory follicular lymphoma. *Ther Adv Hematol*. 2021;12:20406207211015882.

SUPPORTING INFORMATION

Additional supporting information can be found online in the Supporting Information section at the end of this article.

How to cite this article: Kato H, Hayami S, Ueno M, et al. Histone methyltransferase SUV420H1/KMT5B contributes to poor prognosis in hepatocellular carcinoma. *Cancer Sci*. 2024;115:385-400. doi:10.1111/cas.16038